Aust. J. Phys., 1993, **46**, 635–45

Local-field Effects in the High-q-vector Dielectric Response of Si*

T. W. Josefsson and A. E. Smith

Department of Physics, Monash University,
Clayton, Vic. 3168, Australia.

Abstract

The influence of microscopic or local fields on the full frequency- and wavevector-dependent dielectric loss function of Si has been calculated, based on accurate empirical pseudopotential calculations of the electronic structure. It is shown that local-field effects, dramatically significant at optical ($q \approx 0$) wavevectors, diminish with increasing magnitude of q to negligible proportions as q approaches the Brillouin zone boundary. In addition it is shown that the calculated volume-plasmon dispersion relation is improved in comparison with experimental results by the inclusion of local-field effects.

1. Introduction

The high wavevector dielectric response of a solid is of particular interest in electron diffraction and microscopy in relation to inelastic electron scattering (Ritchie and Howie 1977; Smith 1984). The energy lost to a solid by an electron scattering inelastically through single-particle or collective (plasmon) excitation processes may be related to the dielectric function of the solid which depends on both the (Fourier-transformed) complex frequency ω and the wavevector $\boldsymbol{q}$ (Pines 1955; Raether 1980), through the so-called *loss function*

$$\mathrm{Im}\left\{\frac{-1}{\epsilon(\boldsymbol{q},\omega)}\right\}, \tag{1}$$

where $\hbar\boldsymbol{q}$ and $\hbar\omega$ are the momentum and energy transferred to the solid respectively. The general dielectric response of a periodic crystal lattice to an applied external field of frequency ω and wavevector $\boldsymbol{q}$ is to induce rapidly oscillating microscopic or local fields of frequency ω and wavevector $\boldsymbol{q}+\boldsymbol{G}$, where $\boldsymbol{G}$ is a reciprocal-lattice vector. In terms of the Fourier-transformed electric and displacement fields, a *microscopic* dielectric matrix (whose elements are defined in terms of reciprocal-lattice vectors) is defined by

$$\boldsymbol{D}(\boldsymbol{q}+\boldsymbol{G},\omega) = \sum_{\boldsymbol{G}'} \epsilon_{\boldsymbol{G},\boldsymbol{G}'}(\boldsymbol{q},\omega)\,\boldsymbol{E}(\boldsymbol{q}+\boldsymbol{G}',\omega)\,. \tag{2}$$

* Paper presented at the Festschrift Symposium for Dr Geoffrey Fletcher, Monash University, 11 December 1992.

0004-9506/93/050635$05.00

The microscopic local fields (represented by the off-diagonal elements of the dielectric matrix), which oscillate rapidly over the atomic unit cell, are averaged out over several unit cells to give the observable *macroscopic* dielectric function. The macroscopic average is defined in the standard manner as the average of the corresponding microscopic quantity over the primitive unit cell. The macroscopic dielectric function is related to the dielectric matrix through the relation (Wiser 1963)

$$\epsilon(\boldsymbol{q},\omega) = \frac{1}{[\epsilon^{-1}_{\boldsymbol{G},\boldsymbol{G}'}(\boldsymbol{q},\omega)]_{0,0}} \,. \tag{3}$$

That is, the macroscopic dielectric function is the reciprocal of the [0,0] component of the inverse microscopic dielectric matrix, and contains products of the off-diagonal elements of the matrix from the inversion process. In general the presence of the off-diagonal local-field elements implies that

$$\frac{1}{[\epsilon^{-1}_{\boldsymbol{G},\boldsymbol{G}'}(\boldsymbol{q},\omega)]_{0,0}} \neq \epsilon_{0,0}(\boldsymbol{q},\omega) \,. \tag{4}$$

The inclusion of these microscopic or local-field effects is known to improve significantly the calculated optical ($\boldsymbol{q} \approx 0$) loss function of silicon with respect to the experimental optical and electron energy loss data (Louie *et al.* 1975; Cohen and Chelikowsky 1989). However, due to the relative difficulty and time-consuming nature of the accurate evaluation of the dielectric matrix for nonzero $\boldsymbol{q}$ vectors, the influence of local fields at high $\boldsymbol{q}$ has not been considered adequately in previous calculations (Cohen and Chelikowsky 1989; Walter and Cohen 1972). In this work we have for the first time calculated the full frequency- and wavevector-dependent loss function of Si with local-field effects from a complete evaluation of the dielectric matrix. This is based on a very accurate empirical pseudopotential (EPM) calculation of the electronic structure of the solid.

We briefly outline this electronic structure calculation in Section 2, with the loss function calculation proper outlined in Section 3. The results (both with and without local-field effects) for the loss function and the related volume-plasmon dispersion relation are presented for $\boldsymbol{q}$ in the [1,0,0] direction in Section 4.

2. Electronic Structure

The detailed structure in the loss function of the solid is entirely dependent on the electronic structure that we consider. For this reason we have calculated an EPM band structure (Cohen and Chelikowsky 1989) which is inherently more accurate than an *ab initio* calculation (see Wang and Klein 1981) through the use of experimental information in constraining the calculated low-lying bands. We consider the very successful non-local pseudopotential of Chelikowsky and Cohen (1976),

$$V_{\text{pseudo}}(\boldsymbol{r}) = \sum_{\boldsymbol{G}} V_{\boldsymbol{G}}\, S_{\boldsymbol{G}}\, \mathrm{e}^{\mathrm{i}\boldsymbol{G}\cdot\boldsymbol{r}} + \sum_{l=0}^{\infty} A_l(E)\, f_l(\boldsymbol{r})\, P_l \,, \tag{5}$$

where V_G is an adjustable pseudopotential form factor, S_G the usual structure factor, f_l (r) is a function directly simulating the effects of the atomic core states (in our case a square-well potential), P_l is the projection operator for the lth angular momentum state and $A_l(E)$ is an adjustable non-local energy-dependent well depth. In a plane-wave basis we obtain the full non-local pseudopotential Hamiltonian matrix elements as

$$H_{G,G'}(\boldsymbol{k}) = \frac{\hbar^2}{2m}(\boldsymbol{k}-\boldsymbol{G})^2\,\delta_{G,G'} + \sum_{G'} V_{|G'-G|}\cos[(\boldsymbol{G}'-\boldsymbol{G})\,.\,\tau] + \frac{4\pi}{\Omega}\sum_{l} A_l(E)\,(2l+1)\,\mathcal{P}_l(\cos\theta_{G,G'}) \times \int_0^{R_l} j_l(K\,.\,r)\,f_l(r)\,j_l(K'\,.\,r)\,S_{G-G'}\,r^2\,\mathrm{d}r\,, \tag{6}$$

where $\boldsymbol{K} = \boldsymbol{k}+\boldsymbol{G}$, $\mathcal{P}_l(\cos\theta_{K,K'})$ is a Legendre polynomial, R_l is an estimated atomic well width (Animalu and Heine 1965) and $\tau = \frac{1}{8}[1,1,1]$ is the usual diamond structure unit cell origin relative to one of the atoms. The non-local well depth is given in terms of the adjustable parameters α and β by

$$A_l(E) = \alpha_l + \beta_l\,\{[E^0(\boldsymbol{K})\,E^0(\boldsymbol{K}')]^{1/2} - E^0(\boldsymbol{K}_\mathrm{F})\}\,, \tag{7}$$

where $E^0(\boldsymbol{K})$ is the free-electron energy and $E^0(\boldsymbol{K}_\mathrm{F})$ an average energy. For silicon it is necessary to consider only the $l = 0$ angular momentum state and EPM form factor parameters corresponding to the three lowest values of $|\boldsymbol{G}-\boldsymbol{G}'|$ (see Table 1).

Table 1. Empirical pseudopotential parameters (see equations 6 and 7) used for Si

Lattice constant (Å)	$V_{\sqrt{3}}$ (eV)	$V_{\sqrt{8}}$ (eV)	$V_{\sqrt{11}}$ (eV)	α_0 (eV)	β_0 (eV)	R_0 (Å)
5·431	−3·429	−0·517	0·476	7·48	0·32	1·06

Fig. 1 displays the calculated band structure of silicon obtained from this pseudopotential with matrices of the order of 145×145 (the reciprocal-lattice vectors through the set [3,3,3] in units of $2\pi/a$, where a is the unit cell parameter). The four highest valence bands and the 23 lowest conduction bands used in the loss function calculation are shown along the usual symmetry directions in $\boldsymbol{k}$-space.

The initial pseudopotential parameters are based on the Chelikowsky and Cohen (1976) values with minor modifications where needed so that the calculated low-lying bands correspond as closely as possible to experiment. The resulting relative band gaps are within at most 0·05–0·1 eV of the observed values up to the first few conduction bands (Grobman and Eastman 1972; Spicer and Eden 1968; Hulten and Nilsson 1976). The accuracy of the higher bands is more uncertain as experimental results are difficult to obtain (see Fraxedas *et al.* 1990). However, the higher conduction bands are determined completely by the pseudopotential parameters, which in turn are entirely constrained by the very accurate low-lying bands.

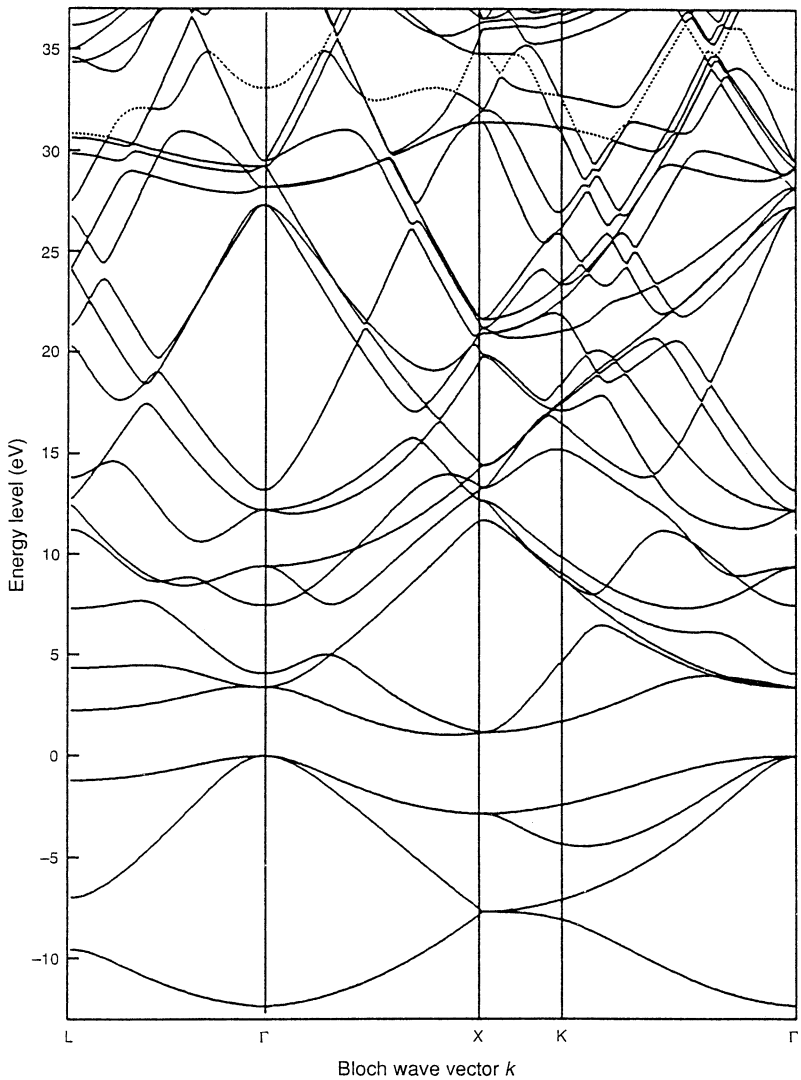

Fig. 1. Electronic structure of silicon calculated in this work. The highest (23rd) conduction band included in the loss function summation is indicated by the dotted line.

3. Dielectric Matrix and Loss Function

An expression for the dielectric matrix in the random phase approximation (RPA) was first derived by Adler (1962) and Wiser (1963):

$$\epsilon_{G,G'}(\boldsymbol{q},\omega) = \delta_{G,G'} - \frac{4\pi e^2}{\Omega|\boldsymbol{q}+\boldsymbol{G}|\,|\boldsymbol{q}+\boldsymbol{G}'|} \times \lim_{\alpha\to 0+} \sum_{\boldsymbol{k},n,n'} \frac{[f_0(E_{n'}(\boldsymbol{k}+\boldsymbol{q})) - f_0(E_n(\boldsymbol{k}))]}{E_{n'}(\boldsymbol{k}+\boldsymbol{q}) - E_n(\boldsymbol{k}) - \hbar\omega + \mathrm{i}\hbar\alpha} \times \langle \boldsymbol{K}+\boldsymbol{q}, n' \,|\, e^{i(q+G')\cdot r} \,|\, \boldsymbol{k}, n\rangle \langle \boldsymbol{k}, n | e^{-i(q+G)\cdot r} \,|\, \boldsymbol{k}+\boldsymbol{q}, n'\rangle\,, \quad (8)$$

where Ω is the system volume, α a 'damping' interaction parameter or self-energy term, ω and $\boldsymbol{q}$ are the frequency and wavevector of the field, $f_0(E)$ the Fermi function, and the summation is over all possible transitions between allowed crystal Bloch states $|\boldsymbol{k}, n\rangle$ with energy $E_n(\boldsymbol{k})$. We rewrite this expression (in the limit of a large crystal) in the integral form

$$\epsilon_{G,G'}(\boldsymbol{q},\omega) = \delta_{GG'} - \frac{4\pi^2}{\Omega|\boldsymbol{q}+\boldsymbol{G}|\,|\boldsymbol{q}+\boldsymbol{G}'|} \sum_{n,n'} G_{n,n'}^{\boldsymbol{G},\boldsymbol{G}'}(\boldsymbol{q},\omega)\,, \tag{9}$$

$$G_{n,n'}^{\boldsymbol{G},\boldsymbol{G}'}(\boldsymbol{q},\omega) = \lim_{\alpha \to 0+} \frac{2}{(2\pi)^3} \int_{\mathrm{BZ}} \frac{F_{n,n'}^{\boldsymbol{G},\boldsymbol{G}'}(\boldsymbol{k},\boldsymbol{q})}{\omega_{n,n'}(\boldsymbol{k},\boldsymbol{q}) - \omega + \mathrm{i}\alpha}\,\mathrm{d}^3\boldsymbol{k}\,, \tag{10}$$

where the band-structure-dependent functions are given by

$$F_{n,n'}^{\boldsymbol{G},\boldsymbol{G}'}(\boldsymbol{k},\boldsymbol{q}) = \langle \boldsymbol{k}+\boldsymbol{q}, n' \,|\mathrm{e}^{\mathrm{i}(q+G)\cdot r}\,|\,\boldsymbol{k}, n\rangle\,\langle \boldsymbol{k}, n\,|\,\mathrm{e}^{-\mathrm{i}(q+G')\cdot r}\,|\,\boldsymbol{k}+\boldsymbol{q}, n'\rangle\,, \tag{11}$$

$$\omega_{n,n'}(\boldsymbol{k},\boldsymbol{q}) = \frac{1}{\hbar}[E_{n'}(\boldsymbol{k}+\boldsymbol{q}) - E_n(\boldsymbol{k})]\,. \tag{12}$$

The functions $F_{n,n'}^{\boldsymbol{G},\boldsymbol{G}'}(\boldsymbol{k},\boldsymbol{q})$ and $\omega_{n,n'}(\boldsymbol{k},\boldsymbol{q})$ must be evaluated numerically by means of time-consuming band structure calculations. In order to decrease the calculation time for the highly singular integral in equation (10), we consider the special points scheme of Monkhurst and Pack (1976). The special points give a much better representation of the complete set of allowed $\boldsymbol{k}$ points than an equivalent number of random points, and may be used to generate orthonormal expansion functions (see Monkhurst and Pack 1976) with the correct symmetry to expand the functions $F_{n,n'}^{\boldsymbol{G},\boldsymbol{G}'}(\boldsymbol{k},\boldsymbol{q})$ and $\omega_{n,n'}(\boldsymbol{k},\boldsymbol{q})$ at an arbitrary point in the Brillouin zone (BZ).

We split the BZ integration into a sum of smaller integrations over mini-cells centred around the special points $\boldsymbol{k}_{\mathrm{c}}$, writing equation (10) (suppressing band, matrix indices and the $\boldsymbol{q}$ dependence for simplicity) as

$$G = \frac{2}{(2\pi)^3} \lim_{\alpha \to 0+} \sum_{k_{\mathrm{c}}} I_{\mathrm{c}}(\boldsymbol{k}_{\mathrm{c}})\,, \tag{13}$$

and expand the band-structure-dependent functions $F_{n,n'}^{\boldsymbol{G},\boldsymbol{G}'}(\boldsymbol{k},\boldsymbol{q})$ and $\omega_{n,n'}(\boldsymbol{k},\boldsymbol{q})$ in a Taylor series to first order:

$$I_{\mathrm{c}}(\boldsymbol{k}_{\mathrm{c}}) \approx \int_{\mathrm{cell\,c}} \frac{F(\boldsymbol{k}_{\mathrm{c}}) - \nabla F(\boldsymbol{k})|_{k_{\mathrm{c}}} \cdot (\boldsymbol{k}-\boldsymbol{k}_{\mathrm{c}})}{\omega(\boldsymbol{k}_{\mathrm{c}}) - \nabla\omega(\boldsymbol{k})|_{k_{\mathrm{c}}} \cdot (\boldsymbol{k}-\boldsymbol{k}_{\mathrm{c}}) - \omega + \mathrm{i}\alpha}\,\mathrm{d}^3\boldsymbol{k}\,. \tag{14}$$

The special points expansion functions of Monkhurst and Pack (1976) are used in conjunction with the analytic Dalton and Gilat (1972) solution to the above integral to obtain an analytic expression for the full integral [equation (10)]. We are only required to perform tedious numerical calculations of $F_{n,n'}^{\boldsymbol{G},\boldsymbol{G}'}(\boldsymbol{k},\boldsymbol{q})$ and $\omega_{n,n'}(\boldsymbol{k},\boldsymbol{q})$ at the few selected special points. The approximations and errors introduced in terminating the Taylor series expansion of the integrand at first

order may be made arbitrarily small by decreasing the mini-cell integration volume or, equivalently, increasing the number of special points. In this sense the accuracy of the full expression (for a given electronic structure) is limited only by the total number of special points we consider.

To obtain satisfactory convergence of the macroscopic dielectric function (from which we obtain the loss function in Section 4), it is sufficient to use 182 special points in the irreducible Brillouin zone (IBZ) or, equivalently, 6912 points in the full BZ. The convergence has been tested with 570 (23328) point calculations in the IBZ (BZ), and the results differ by less than a few per cent. In addition it is necessary to consider dielectric matrices of the order of 59×59 in the inversion process, corresponding to all those reciprocal-lattice vectors $\boldsymbol{G}$ through the set [2,2,2] (in units of $2\pi/a$).

The symmetry of the dielectric matrix may be used to further simplify the calculation process considerably. Although $\epsilon_{\boldsymbol{G},\boldsymbol{G}'}(\boldsymbol{q},\omega)$ is hermitian, its symmetry is in general quite complicated and is related to the wavevector $\boldsymbol{q}$ and the lattice symmetry through the symmetry of $F^{\boldsymbol{G},\boldsymbol{G}'}_{n,n'}(\boldsymbol{k},\boldsymbol{q})$ and $\omega_{n,n'}(\boldsymbol{k},\boldsymbol{q})$. For the $\boldsymbol{q}=0$ case the dielectric matrix has the full symmetry of the crystal lattice; we need

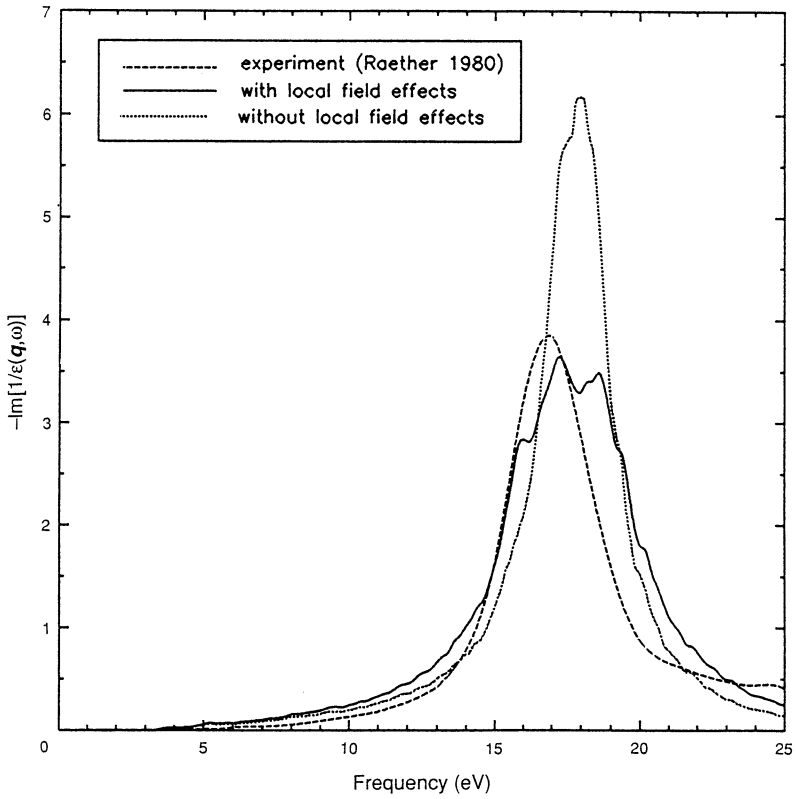

Fig. 2. Calculated (570 special points) and experimental optical ($\boldsymbol{q}=0$) loss function for Si around the plasmon peak.

only consider the 1/48 irreducible wedge of the BZ (182 k points in the integrations) and 72 independent terms in the dielectric matrix. In the next section we present results for finite q in the [1,0,0] direction, where the symmetry is more complicated. The 182 special points result in 963 independent sets of k and $k+q$ points in the integrations. In addition there are now 225 independent terms in the dielectric matrix.

4. Results and Discussion

The calculated optical $q \to 0$ loss function for Si is dramatically improved in comparison with experimental results by the inclusion of local-field effects as first shown by Louie *et al.* (1975). In Fig. 2 we compare the present $q \to 0$ results (from a 570-special-point calculation) with and without local-field effects, with the experimental results (Raether 1980).

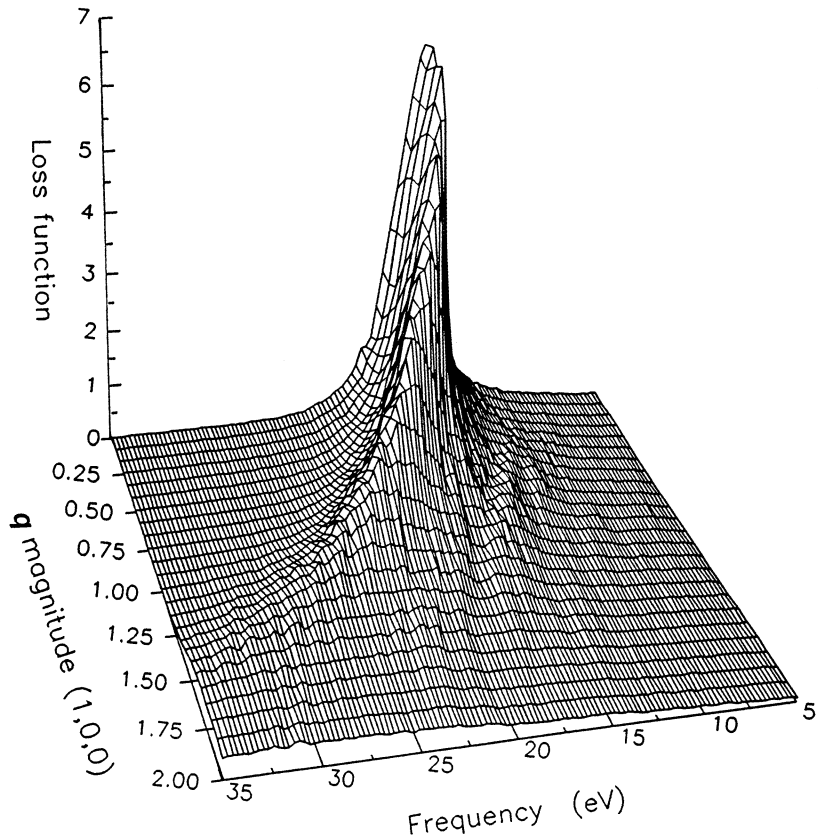

Fig. 3. Calculated (182 special points) loss function for Si without local-field effects for $q = 0$ to [2,0,0] in units of $2\pi/a$.

The main plasmon peak centred at 17·9 eV without local-field effects is shifted down to 17·2 eV, only 0·3 eV above the 16·9 eV experimental plasma frequency. In addition the magnitude of the plasma peak is reduced by almost half, indicating that collective electron or plasmon excitations are less well defined in the presence of the rapidly oscillating microscopic fields. The agreement between experiment and theory (see Fig. 2) is very good, considering that electron exchange, correlation effects and electron–hole interactions are not considered directly in the RPA (see Van Camp *et al.* 1981) or in our band structure calculation (see Hybertson and Louie 1984; Manghi *et al.* 1985). This is partly due to the fact that the dielectric function at the higher frequencies, where the loss function peak occurs, is much less dependent on the low-lying energy levels, where electron–hole effects are significant, than on the higher energy bands where these effects are less important. The detailed structure in the loss function above 15 eV is dependent on (and hence a measure of) the high-lying band structure topology.

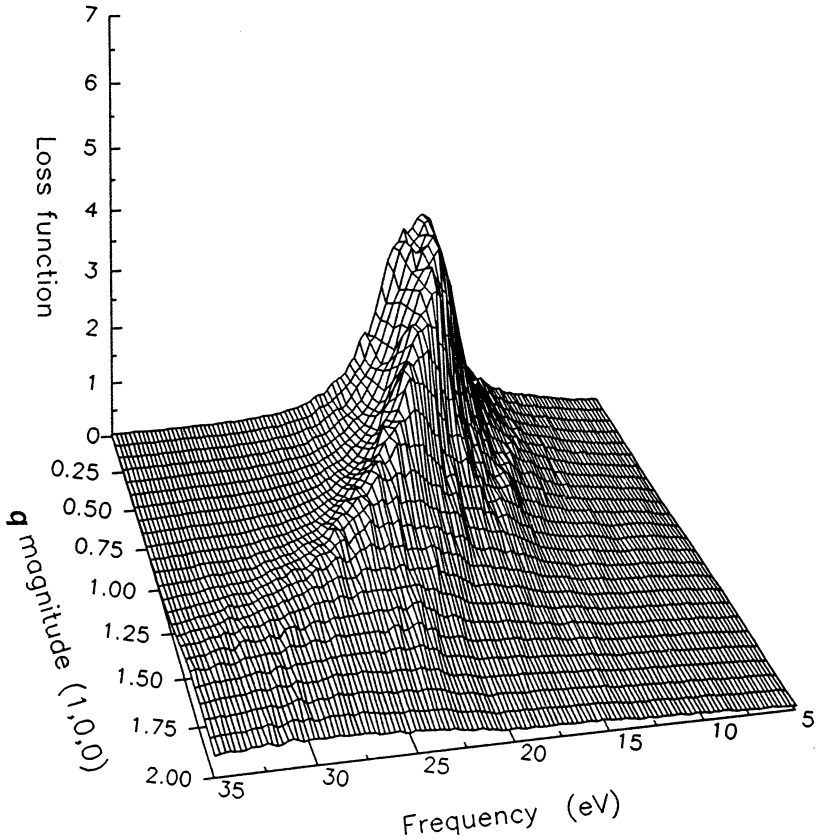

Fig. 4. Calculated (182 special points) loss function for Si including local-field effects for $q = 0$ to [2,0,0] in units of $2\pi/a$. The loss function above $q \approx$ [1,0,0] is very similar to Fig. 3.

With increasing magnitude of q the plasma frequency shifts to higher energies (see Figs 3 and 4 for q ranging from 0 through to [2,0,0]) and, contrary to previous work [performed without local-field effects: Cohen and Chelikowsky (1989); Walter and Cohen (1972)], the loss function peak broadens and the magnitude decreases. Above $q = [2,0,0]$ the loss function peak becomes very broad, indicating that collective electronic or plasmon excitations are very weak and not sustainable.

The effect of the rapidly oscillating microscopic fields decreases quickly as the magnitude of q increases, to the extent that the dramatic effect observed on the plasmon peak at $q = 0$ (Fig. 2) is almost negligible as q approaches the Brillouin zone boundary (see Fig. 5). This indicates that rapidly varying microscopic fields are also unsustainable at these high wavevectors.

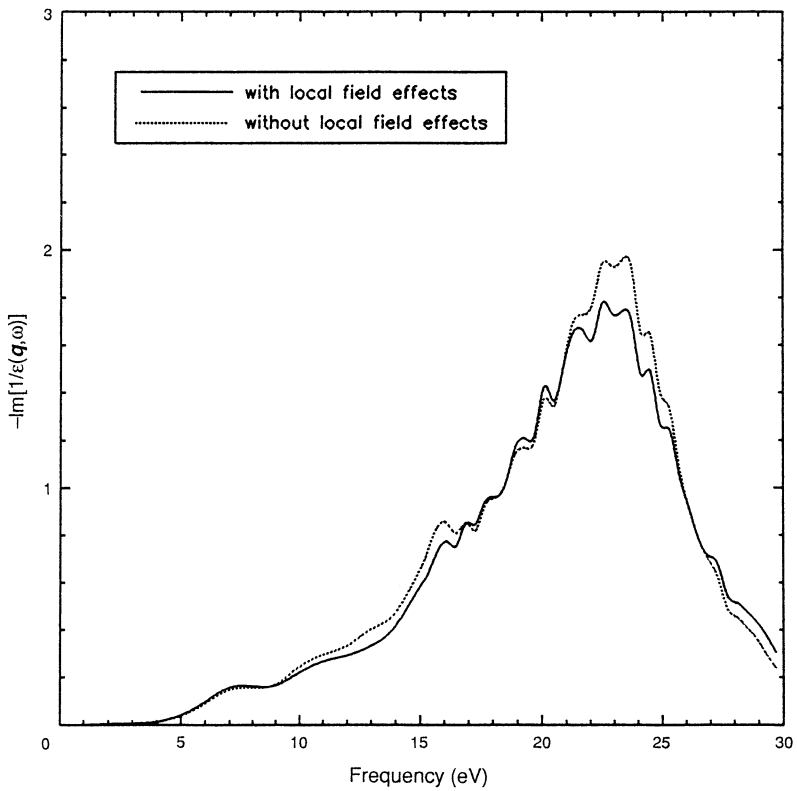

Fig. 5. Calculated (570 special points) loss function with and without local-field effects for Si around the plasmon peak. Here $q = [1,0,0]$ in units of $2\pi/a$.

The loss function peak is a measure of collective longitudinal excitations (volume-plasmons) in the solid (Raether 1980). Fig. 6 displays the loss function peak frequency versus wavevector or the volume-plasmon dispersion relation. Results both with and without local-field effects are compared with the experimental results of Stiebling and Raether (1978). It can be seen that consideration of the local fields considerably improves the calculated dispersion relation at small

q, but the effect diminishes with increasing q. The parabolic nature of the calculated and experimental dispersion relations is shown up to the Brillouin zone boundary $q = [1,0,0]$. Beyond this point the calculated results become too broad to define any clear plasma frequency. However, the RPA results do not seem to taper off to the extent that the experimental results do. This is not related to local-field effects (or poor band structure) but is most likely due to the neglect of Landau damping of the plasmons (Bross 1978).

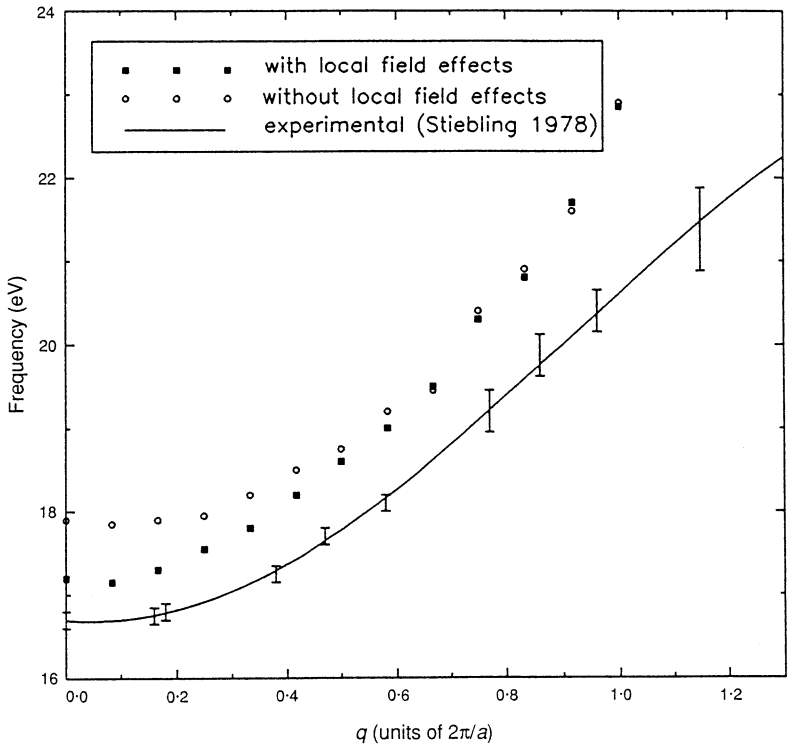

Fig. 6. Calculated plasmon dispersion relation with (solid squares) and without (open circles) local-field effects. The experimental results (Stiebling and Raether 1978, solid curve) are also shown.

5. Conclusion

For small optical wavevectors q it is known (Louie *et al.* 1975; Cohen and Chelikowsky 1989) that rapidly varying microscopic or local fields dramatically improve the electron energy loss function as calculated from the dielectric response in the RPA. The calculated plasma frequency with local-field effects is decreased by 1 eV to 17·2 eV, approaching the experimental frequency of 16·9 eV. The experimental plasmon peak magnitude is also accurately reproduced. This reduction in the calculated plasmon peak height (by a factor of two) indicates

that local-field effects result in less well defined collective electronic or plasmon excitations. We have calculated accurately for the first time the large-q-vector dependence of the loss function, including the effects of rapidly oscillating microscopic fields. It has been shown that these local fields become progressively less significant as the magnitude of q increases, to the extent that they are almost negligible as q approaches the Brillouin zone boundary. For this reason the inclusion of local-field effects, while significantly improving the small-q plasmon dispersion relation, does not affect the large-q dispersion relation to the same extent.

Acknowledgments

One of us (T. W. Josefsson) acknowledges the receipt of an APRA scholarship towards the completion of doctoral studies at Monash University.

References

Adler, S. (1962). *Phys. Rev.* **126**, 413.
Animalu, A. O. E., and Heine, V. (1965). *Philos. Mag.* **12**, 1249.
Bross, H. (1978). *Phys. Lett.* A **64**, 418.
Chelikowsky, J. R., and Cohen, M. L. (1976). *Phys. Rev.* B **14**, 556.
Cohen, M. L., and Chelikowsky, J. R. (1989). 'Electronic Structure and Optical Properties of Semiconducters' (Springer: Berlin).
Dalton, N. W., and Gilat, G. (1972). *Solid State Commun.* **10**, 287.
Fraxedas, J., Stampfl, A., Leckey, R. C. G., Riley, J. D., and Ley, L. (1990). *Phys. Rev.* B **42**, 8966.
Grobman, W. D., and Eastman, D. E. (1972). *Phys. Rev. Lett.* **29**, 1508.
Hulten, R., and Nilsson, N. G. (1976). *Solid State Commun.* **18**, 1341.
Hybertson, M. S., and Louie, S. G. (1984). *Phys. Rev.* B **30**, 5777.
Louie, S. G., Chelikowsky, J. R., and Cohen, M. L. (1975). *Phys. Rev. Lett.* **34**, 155.
Manghi, F., Riegler, G., and Bertoni, C. M. (1985). *Phys. Rev.* B **31**, 368.
Monkhurst, H. J., and Pack, J. D. (1976). *Phys. Rev.* B **13**, 518.
Pines, D. (1955). *In* 'Solid State Physics' (Eds F. Seitz and D. Turnbull), Vol. 1 (Academic: New York).
Raether, H. (1980). 'Excitations of Plasmons and Interband Transitions by Electrons' (Springer: New York).
Ritchie, R. H., and Howie, A. (1977). *Philos Mag.* **36**, 463.
Smith, A. E. (1984). *Phys. Status Solidi* B **123**, 619.
Spicer, W. E., and Eden, R. C. (1968). Proc. Ninth Int. Conf. on the Physics of Semiconductors, Moscow 1968 (Nauka: Leningrad).
Stiebling, J., and Raether, H. (1978). *Phys. Rev. Lett.* **40**, 1293.
Van Camp, P. E., *et al.* (1981). *Phys. Rev* B **24**, 1096.
Walter, J. P., and Cohen, M. L. (1972). *Phys. Rev.* B **5**, 3101.
Wang, C. S., and Klein, B. M. (1981). *Phys. Rev.* B **24**, 3417.
Wiser, N. (1963). *Phys. Rev.* **129**, 62.

Manuscript received 21 January, accepted 27 April 1993